

---

# INFORMATION EVOLUTION IN COMPLEX NETWORKS

---

A PREPRINT

**Yang Tian**

Department of Psychology & Tsinghua Laboratory of Brain and Intelligence  
Tsinghua University  
Beijing, 100084, China.  
tiany20@mails.tsinghua.edu.cn

**Justin L. Gardner**

Department of Psychology  
Stanford University  
Stanford, CA 94305, USA  
jlg@stanford.edu

**Guoqi Li**

Department of Precision Instrumentation & Center for Brain Inspired Computing Research  
Tsinghua University  
Beijing 100084, China  
liguoqi@mail.tsinghua.edu.cn

**Pei Sun**

Department of Psychology & Tsinghua Laboratory of Brain and Intelligence  
Tsinghua University  
Beijing, 100084, China.  
peisun@tsinghua.edu.cn

November 15, 2021

## ABSTRACT

Many biological phenomena or social events critically depend on how information evolves in complex networks. A seeming paradox of the information evolution is the coexistence of local randomness, manifested as the stochastic distortion of information content during individual-individual diffusion, and global regularity, illustrated by specific non-random patterns of information content on the network scale. The current research pursues to understand the underlying mechanisms of such coexistence. Applying network dynamics and information theory, we discover that a certain amount of information, determined by the selectivity of networks to the input information, frequently survives from random distortion. Other information will inevitably experience distortion or dissipation, whose speeds are shaped by the diversity of information selectivity in networks. The discovered laws exist irrespective of noise, but the noise accounts for their intensification. We further demonstrate the ubiquity of our discovered laws by applying them to analyze the emergence of neural tuning properties in the primary visual and medial temporal cortices of animal brains and the emergence of extreme opinions in social networks.

## 1 Introduction

Information diffusion, as the name suggests, describes the spreading of information (e.g., viral memes or rumors) among individuals in complex networks [49]. Challenge topics in various disciplines, such as communications, collective actions, and public sentiments, can be abstracted as information diffusion [19, 35, 6, 11, 5]. Rooted in physics [16, 30, 31, 4], the study of information diffusion has seen fruitful applications in biological and social sciences as well [17, 38, 32, 25, 29].

Despite the substantial progress, there are still numerous problems unsolved in this emerging direction [49]. Among these problems, a critical one is about information evolution, a phenomenon referring to the dynamic variation of information content during its diffusion. Although information evolution is widespread in various complex systems,

much unknown remains about its underlying mechanism. While some obstacles arise from the inapplicability of existing information diffusion models (e.g., percolation) that treat information as an entirety rather than a compound of contents [11, 16, 17, 18, 37, 47, 23, 39, 10, 7], more essential problems lie in a seeming paradox of information evolution: some regular global patterns of information evolution can naturally emerge from and robustly coexist with the random distortion of information during local individual-individual diffusion (e.g., the random distortion studied by Shannon [40]), irrespective of whether individuals tend to create such regularity or not. It is elusive how local random distortions ultimately lead to global regularity rather than accumulate to utter disorder, especially when individuals' tendency or strategy is absent. Such spontaneous global regularities, frequently observed when information diffuses in real complex networks (e.g., the hierarchical representation of visual information in the brain [22, 46]), may originate from specific undiscovered laws governing information evolution.

The current research pursues to formalize information evolution based on a combination of network dynamics and information theory. We attempt to explore global laws governing information evolution during its diffusion and study their coexistence with local random distortion. By generalizing our theory into representative complex networks, we demonstrate the fundamental role of the discovered laws in shaping various biological and social phenomena.

## 2 Information evolution during diffusion

To understand how information content might evolve, let us consider the information diffusion in a complex network (see details in Appendix A). As a basic network unit, each individual has multiple possible responses that vary depending on the received information (referred to as information selectivity). Any input information will trigger an information diffusion process where each individual receives information from upstream individuals and passes on its response to subsequent individuals (e.g., **Fig. 1b** or **Fig. 1c**). Meanwhile, individuals attempt to learn about (estimate) the factual input information based on what they received. For any information, its content is principally a symbol sequence. After receiving symbol  $s'$ , the probability for individual  $i$  to respond by  $s$  is  $\mathcal{P}_i(s | s')$ . This conditional probability distribution describes the information selectivity of individual  $i$  (**Fig. 1a**). As suggested by Shannon [40], an interesting situation will occur when more than one conditional probability quantity (e.g.,  $\mathcal{P}_i(s | s')$  and  $\mathcal{P}_i(s | s'')$ ) is non-zero given different received information  $s'$  and  $s''$  (**Fig. 1a**). In this situation, there is no bijective mapping between the received information and the corresponding response. Symbol  $s'$  may be recognized as symbol  $s''$  since their responses are same. This situation is referred to as information confusion in information theory [40]. Apart from the above probabilistic description, we can also represent information confusion utilizing the confusion graph (CG) on symbol set  $S$  [40, 28, 2]. Specifically, we treat symbols as the nodes in graph  $\mathcal{G}(S)$  and define an edge between two nodes only if they are confused with each other (**Fig. 1a**). More details are provided in Appendix B.

Given these foundations, let us return to the question on how information content evolves during the diffusion process. One can consider a case where information confusion happens on individual  $i$ , and then the response of individual  $i$  (referred to as representational information) is passed on to individual  $j$ . To get knowledge of the factual information received by individual  $i$ , individual  $j$  needs to decode the representational information from individual  $i$ . When information confusion happens on individual  $i$ , the dilemma faced by individual  $j$  is that one representational information corresponds to more than one possibility of factual information (**Fig. 1a**). This one-to-many mapping may make individual  $j$  misestimate the factual information. Therefore, the factual information in individuals' knowledge may change when confusion happens (see Appendix C). In **Fig. 1b**, we show an example of information evolution. One can see how the information content is gradually distorted from the factual state "It is a cat" during diffusion. We refer to this phenomenon as information distortion. In **Fig. 1c**, we implement a more realistic and larger experiment. We consider two kinds of information diffusion. The first one requires the information selectivity of every individual to be completely known (noise-free case, which represents the ideal diffusion), while the second one does not (i.e., noisy case, which corresponds to the information diffusion in more realistic situations). One can realize the similarity between these settings and the complete/incomplete information conditions. During the diffusion, we quantify the content variation utilizing the Hamming distance [21]. We observe a continuous increase of information content changes along the diffusion pathways, which is independent of noise. However, the existence of noise accounts for accelerating information distortion (**Fig. 1c**).

Information dissipation, a special case of distortion, is another notable phenomenon during diffusion. We define dissipation as the process where the maximum number of symbols that possibly occur in the diffused information, or the maximum information quantities possibly contained in the diffused information, decreases along the diffusion pathway (see Appendix D). In **Fig. 1d**, we make all symbols in  $S$  (Latin letters) uniformly distributed in the input information. When this information diffuses in a complex network with information confusion, information dissipation naturally emerges. One can verify this finding through symbol counting or information quantity measurement and observe its independence of noise. As expected, noise accelerates the dissipation process as well.

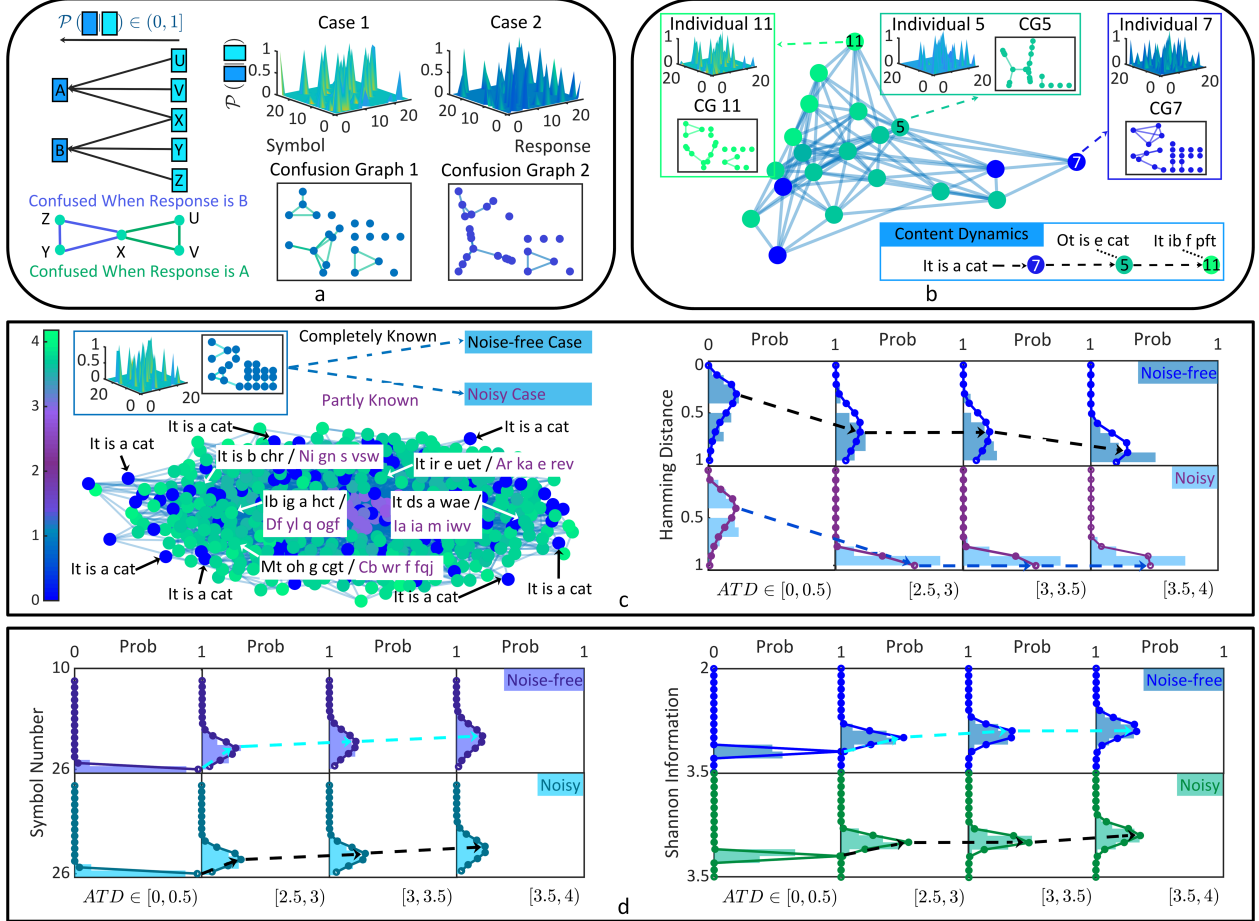


**Figure 1: Information evolution during diffusion.** **a**, We illustrate an example where the confusion relations in  $\{U, V, X\}$  or  $\{X, Y, Z\}$  occur when the response is  $A$  or  $B$ , respectively (left). We also show two instances of confusion graphs (middle and right). **b**, The information content evolves from the factual state “It is a cat” to other distorted states in a diffusion path  $7 \rightarrow 5 \rightarrow 11$ . **c**, In a network of 500 individuals (color represents the average time delay (ATD) of receiving information), we set two kinds of diffusion: noise-free case (the black words in white boxes) and noisy case (the purple words in white boxes). One can find more significant information distortion in the noisy case (left). The Hamming distance between diffused information and factual information quantifies the information content variation, whose probability distribution (sampled from all individuals) gradually approaches 1 as ATD increases. Moreover, this approaching process is sharper in the noisy diffusion than the noise-free one (right). **d**, We set a piece of new information for the complex network in **Fig. 1c**, where 26 Latin letters are uniformly distributed. The maximum number of the letters that possibly occur in the diffused information (left) and the Shannon entropy of the letter probability distribution (right) decrease with the time delay (diffusion distance), demonstrating the information dissipation.

In summary, the above experiments demonstrate that information distortion and dissipation inevitably happen once there is information confusion during diffusion. This phenomenon occurs even during the noise-free diffusion process and is intensified if noise exists.

### 3 Invariants in information evolution

Let us move on to the central question about the global laws governing information evolution. A possible law may be discovered by analyzing what is invariant during information diffusion, irrespective of the distortion and dissipation observed above. In other words, we wonder what kind of information will not be distorted or dissipated in a given diffusion process. Because information distortion and dissipation inevitably result from information confusion, our question can be solved by measuring the maximum amount of information contents that diffuse without confusion.

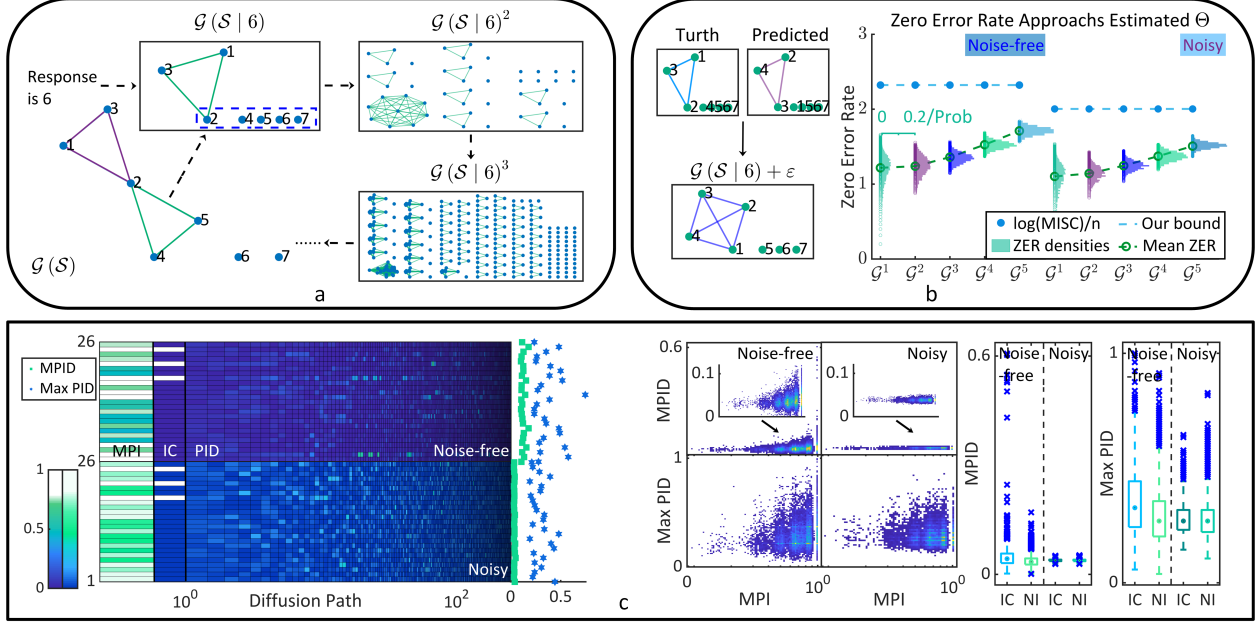


**Figure 2: Invariants in information evolution.** **a**, We show the confusion graph  $\mathcal{G}(\mathcal{S})$  on a hypothetical symbol set  $\mathcal{S}$  of 7 symbols. Then we show the reconstructed confusion graph  $\mathcal{G}(\mathcal{S}|6)$  and its graph products. **b**, We illustrate the generation of  $\mathcal{G}(\mathcal{S}) + \varepsilon$  given the ground truth graph and the predicted graph. Then, we demonstrate the validity and optimality of the bound in (2) by comparing it with the maximum zero error rate obtained by maximum independent set searching ( $\log(\text{MISC})/n$ ). After the random sampling for independent sets, one can see the approaching tendency of these random sampled zero error rates (ZER) to our predicted bound (both the densities and mean value). **c**, A piece of information (26 Latin letters are uniformly distributed) diffuses in a chain of 200 individuals 500 times (see an instance in the left part). Each time the information selectivity of individuals is randomized, determining the independent set of confusion graphs and corresponding information invariants. We show that the mean probability for letter  $s$  to be an invariant for every individual (MPI) positively modifies the mean/max probability for  $s$  to occur in the diffused information content (MPID/Max PID). Letters that belong to the shared invariant content set of all individuals (IC) have higher MPID/Max PID values than the letters out of the common invariant content set (NI).

Following this idea, we analyze a general case where individual  $i + 1$  receives information  $I_i = (s_1^i, \dots, s_l^i)$  from individual  $i$  and attempts to learn (or estimate) the factual information. The estimation necessarily requires to get knowledge of the information selectivity of individual  $i$  (e.g.,  $\mathcal{P}_i(\cdot | \cdot)$  or  $\mathcal{G}_i(\mathcal{S})$ ). From a graphical perspective, this estimation corresponds to a subdivided reconstruction process of confusion graph  $\mathcal{G}_i(\mathcal{S})$ . Individual  $i + 1$  needs to reconstruct a possible connected component where any two nodes (symbols) are confused when the response is  $s_j^i$ . The rest nodes excluded in this connected component are treated as isolated since response  $s_j^i$  has no constraint on their confusion relations (Supplementary Section 4). This reconstructed graph is referred to as  $\mathcal{G}_i(\mathcal{S} | s_j^i)$ , whose independence number  $\alpha$  (cardinality of the largest independent set) is the maximum amount of the symbols that will not be confused given a response  $s_j^i$  (Fig. 2a).

Applying the graph product  $\boxtimes$ , we can generalize the confusion graph of single symbols to the confusion graph of the strings of length  $n$  [40]. We implement the graph product  $n - 1$  times to obtain  $\mathcal{G}_i(\mathcal{S} | s_j^i)^n = \mathcal{G}_i(\mathcal{S} | s_j^i) \boxtimes \dots \boxtimes \mathcal{G}_i(\mathcal{S} | s_j^i)$  (Fig. 2a). This generalization helps formulate the maximum amount of information (no matter it is a symbol or a string) that can diffuse from individual  $i$  to individual  $i + 1$  without confusion given a response  $s_j^i$

$$\Theta(i \rightarrow i + 1 | s_j^i) = \sup_{n \in \mathbb{N}} \log \sqrt[n]{\alpha[(\mathcal{G}_i(\mathcal{S} | s_j^i) + \varepsilon)^n]}, \quad (1)$$

where  $\varepsilon$  measures the noise and vanishes in the noise-free case. The reconstruct graph  $\mathcal{G}_i(\mathcal{S} | s_j^i) + \varepsilon$  (see details in Fig. 2b and Appendix E) inherits the topology of the ground truth  $\mathcal{G}_i(\mathcal{S} | s_j^i)$  (since it indeed exists and shapes information diffusion) and the prediction of  $\mathcal{G}_i(\mathcal{S} | s_j^i)$  by individual  $i + 1$  (since it affects the action pattern of individual  $i + 1$ ). Apart from that, one can also learn the basic form of equation (1) in Shannon's work [40].

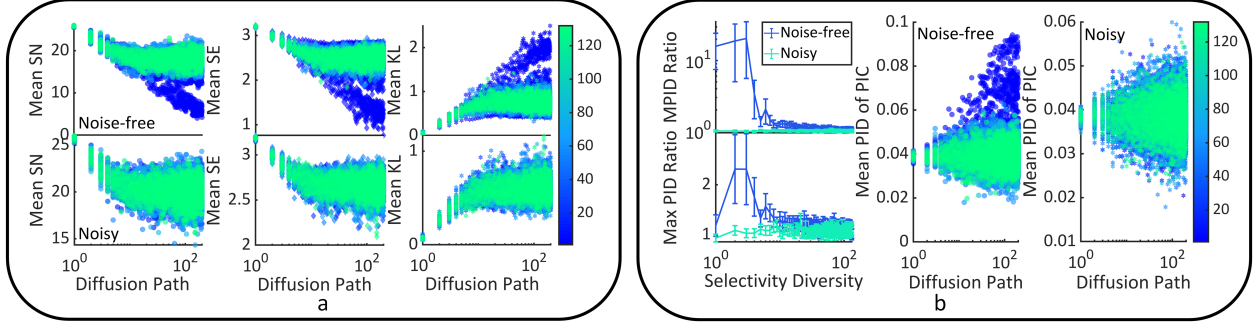


**Figure 3: Information selectivity diversity shapes information evolution and the convergence to invariants.** **a,** We repeat the experiment in **Fig. 3c** 1000 times. Each time there exist  $n$  kinds of information selectivity in the network ( $n \in [1, 140]$  is randomized). We visualize the information distortion (KL divergence between the original and the diffused symbol distributions) and dissipation (symbol number “SN” and Shannon entropy “SE”) along the diffusion pathway (the colors of data points scale according to  $n$ ). **b,** We generalize the scope of IC and define the potential information invariants (PIC) as the letters whose MPI values are above average. After measuring the ratios of MPID/Max PID between the letters in PIC and the letters out of PIC, we analyze these ratios as the functions of selectivity diversity  $n$  (left). Note that error bars denote a quarter of the standard deviations. Moreover, we calculate the probability for a symbol to occur in the diffused information content (PID) and analyze the mean PID of the symbols in PIC during diffusion (middle and right).

A critical challenge concerning equation (1) is how to calculate  $\Theta$ . On the one hand, Shannon has suggested the difficulty of developing an analytical calculation [40]. On the other hand, obstacles emerge inevitably in computational attempts because  $\alpha$  is  $NP$ -hard to compute [26]. To overcome this challenge, we build on Shannon’s work [40] to estimate the upper bound of  $\Theta$ . Given that  $\alpha$  is bound by the maximum clique value  $\lambda$  of the graph following  $\alpha \leq \lambda^{-1}$ , one can further prove  $\log \sqrt[n]{\alpha(\cdot)} \leq \log \lambda^{-1}(\cdot)$ . Moreover, exploiting that every connected component of  $(\mathcal{G}_i(\mathcal{S} | s_j^i) + \varepsilon)^n$  ( $n \in \mathbb{N}$ ) is a clique (since the confusion relation given a response is an equivalence relation and has transitivity, see **Fig. 2a-b**), we can obtain

$$\Theta \leq \log \left[ \frac{\theta + \theta \sum_s (1 - \tau_s)}{\mu} \right]^\omega |\mathcal{S}|^{(1-\omega)}, \quad (2)$$

where notion  $\tau_s = \mathcal{U}[\deg(s)]$  traverses all nodes in graph  $\mathcal{G}_i(\mathcal{S} | s_j^i) + \varepsilon$  (here  $\mathcal{U}(\cdot)$  is the unit step function). And we mark that  $\omega = \mathcal{U}(\sum_s \tau_s)$ . Moreover, we pick one node that has minimum degree in the graph. Then  $\mu$  measures the number of the cliques that contain this node and  $\theta$  counts the cliques in the same connected component with this node (Appendix F).

In **Fig. 2b**, the proposed bound is computationally validated by being compared with the maximum zero error (non-confusion) information rate obtained by maximum independent set searching (the Bron–Kerbosch algorithm [8, 3]). It is easy to verify the correspondence between these two results. Furthermore, our bound is mathematically proven as a supremum when the confusion graph is not complete. In the opposite case,  $\Theta = 0$  can be directly obtained, making the upper bound estimation unnecessary (see Supplementary Section 5). Apart from the verification, we also implement random sampling for independent sets in each graph  $10^5$  times, calculating zero error rate samples. Consistent with Shannon’s prediction, these samples approach the upper bound as the graph product order increases.

To this point, we can conclude that information invariants are the information quantities that have not exceed the upper bound of  $\Theta$ . Noise can intensify distortion and dissipation as the bound in  $\mathcal{G}_i(\mathcal{S} | s_j^i) + \varepsilon$  is no more than that in  $\mathcal{G}_i(\mathcal{S} | s_j^i)$  (Supplementary Section 5). In **Fig. 2c**, we show that information invariants are more likely to be maintained during the diffusion process, yet noise can disrupt the process.

Furthermore, inspired by the fact that information confusion is determined by the information selectivity of individuals, we hypothesize that the diversity of information selectivity in the network plays a pivotal role in shaping information distortion, dissipation, and the convergence to invariants. The results shown in **Fig. 3** confirm our hypothesis. One can find more significant information distortion and dissipation when the information selectivity is more monotonous (**Fig. 3a**). Information invariants will occupy most parts of the diffused information content, implying a large ratio between the proportions of invariant contents (high proportion) and other contents (low proportion) in the diffused information (**Fig. 3b**). The increasing diversity of information selectivity will mitigate this process. Meanwhile, the effects of diversity will vanish due to the disturbance of noise (**Fig. 3**).

In sum, our potential laws of information evolution suggest that specific information invariants frequently survive from random distortion during diffusion. These invariants create regularity on a network scale as they gradually dominate the information content, coexisting with the random distortion during individual-individual diffusion. As for the information contents that are not invariants, their distortion and dissipation are inevitable and shaped by the diversity of information selectivity in networks.

## 4 Information evolution in biological and social systems

The above laws are discovered through an abstract information diffusion model. Below we turn to measure information diffusion in realistic complex networks to build possible connections between our laws and biological or social phenomena.

An example of biological system considered here is the neural pathway from the primary visual cortex (V1) to the middle temporal visual cortex (MT) in the animal brain. These two cortices are responsible for processing the orientation, direction and motion information of visual stimuli [44]. During the information diffusion from V1 to MT, a remarkable phenomenon is that the neural selectivity (a kind of information selectivity that governs neural activity profile) changes from the selectivity of the velocity component orthogonal to the preferred spatial orientation (simple and complex neurons in V1 [1]) to the selectivity of velocity entirety (MT neurons [36]). This variation accounts for the subdivided and staged neural representation of motion information [36]. Computationally, Simoncelli and Heeger simulate the above process in a layered neural cluster model [43, 41, 42]. This model is generalized and experimentally-validated in a subsequent study [36]. Here we pursue to study how the modeled phenomenon naturally emerges from neural collective dynamics during information diffusion.

In **Fig. 4a**, we consider a tripartite neural cluster that is not strictly layered. The synaptic connections in this cluster are randomized. We characterize stimulus-triggered neural activities utilizing a non-homogeneous stochastic neural network [45]. This framework can generate variable neural activities governed by both neural selectivity and network dynamics. In the characterization, we only preset the neural selectivity of simple neurons to affect (not completely control) their activity profiles. Consistent with previous experimental studies [34, 33], the selectivity of each simple neuron is described by a triangular orientation tuning curve. There is no preset limitation for complex and MT neurons, providing an opportunity to explore how the characteristics of their activities emerge. We set a long enough stimulus sequence where each stimulus is a velocity vector (see Appendix G for experiment settings). In **Fig. 4b**, we show the observed tuning curve of complex and MT neurons. Mathematically, we quantify how “narrow” or “broad” the neural selectivity is based on the variance of the normalized neural response rates for every stimulus. One can see the broadening of neural selectivity during the information diffusion from the V1 cortex to the MT cortex. To understand this phenomenon, we calculate the upper bound of  $\Theta$  for each neuron based on (2). Meanwhile, we also measure the determinability rate variance of complex neurons and MT neurons, which principally quantifies the capacity of the diffusion paths from simple neurons to each complex or MT neuron to resist information distortion (see Appendix G). Experimental results show that a neuron with higher response variance will also have a larger upper bound of  $\Theta$ , meaning that a neuron with a higher selectivity degree can pass on more undistorted information content. Moreover, a complex neuron or MT neuron that receives the information content with more distortion will have a lower selectivity degree because the determinability rate variance modifies the response variance positively. To conclude, these results suggest a possibility that the variation of neural selectivity from the V1 cortex to the MT cortex originates from the information distortion along the neural pathway.

The social phenomenon of interest to this research is the polarization of opinions in multi-agent interactions. Here we implement the analysis based on the opinion concerning credit. In realistic financial, marketing, and other social activities, agents may do selfish (e.g., lie or cheat) or even spiteful (e.g., break rules for non-interest reasons) behaviors to make profits or harm others [20, 15]. These behaviors are costly [14], leading to a series of punishments. Among these punishments, the damage on credit and reputation is of interest for theoretical and practical reasons [48, 24]. A widespread phenomenon concerning credit damage is the emergence of extreme views towards the credit of an agent. The opinions on one’s credit might be polarized when credit information diffuses [12]. Although the agent occasionally does selfish or spiteful behaviors, its credit in others’ view may still approach extraordinarily high or extremely low. This phenomenon might be caused by both psychological and physical factors [12, 27]. Here we explore whether information diffusion characteristics alone are sufficient to polarize the opinions on credit.

We consider a situation where agent  $i$  does selfish or spiteful behaviors with probability of  $p'$  or  $p''$  in a  $l$ -run game, respectively. Several randomly selected agents observe the game and spread the credit information. The spread information contains the credit records in every run, determining whether agent  $i$  will be treated as selfish, spiteful, or amicable (see Appendix H for settings). In **Fig. 5a**, we illustrate the polarization process of the opinion on the credit of agent  $i$  along the diffusion pathway (each agent’s opinion is the corresponding estimated factual information). Here

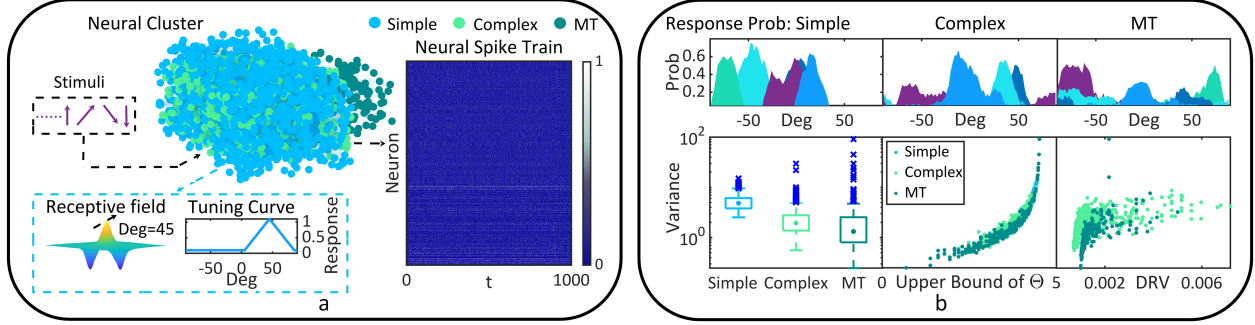


**Figure 4: Information evolution in biological systems.** **a**, A neural cluster receives a random stimulus sequence and generates spikes. The receptive field and neural selectivity are merely preset for simple neurons. **b**, We respectively illustrate 5 examples of  $P$  (Response | Stimulus) for each kind of neurons. Consistent with previous studies [34, 33], the variance of normalized neural response rates decreases from simple neurons to MT neurons. Moreover, we demonstrate that the upper bound of  $\Theta$  correlates to the response variance of all neuron types positively, while the determinability rate variance (DRV) modifies the response variance of each complex or MT neuron positively.

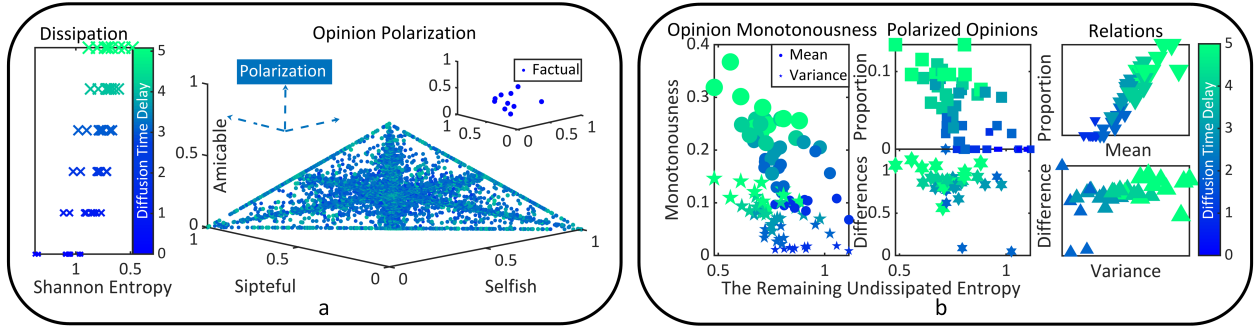


**Figure 5: Information evolution in social systems.** **a**, A credit information diffusion experiment runs 10 times. Each time a random credit information begins to diffuse from several random agents. We show that the opinion polarization concerning the credit of agent  $i$  happens along with information dissipation. **b**, We quantify the polarization degree utilizing the monotonousness of opinions (left). One can find that opinions become more monotonous during dissipation (see “Mean”), and the differences between different agents’ opinion monotonousness quantities gradually increase (see “Variance”). Meanwhile, similar escalating trends can be seen in the proportion of extreme opinions among all opinions and the differences between these extreme opinions (middle). Therefore, the polarization of opinions (“Mean” and the proportion of extreme opinions) emerges during dissipation and enlarges the opinion differences (“Variance” and the differences between extreme opinions) between agents (right).

the diffusion process is set as noisy to fit in with realistic situations. During information distortion and dissipation, the probability for agent  $i$  to do selfish or spiteful behaviors in the game is driven farther from  $p'$  or  $p''$ . It gradually approaches 0 or 1, suggesting that the opinion on the credit of agent  $i$  is polarized. In Fig. 5b, we quantify the polarization degree of opinions and attempt to measure the proportion of extreme opinions among all opinions (see Appendix H). These quantitative results demonstrate that opinions are polarized along with information dissipation, during which extreme opinions naturally emerge. Meanwhile, one can see the increasing differences between different extreme opinions, suggesting the intensified disagreements between agents. In summary, the characteristics of information diffusion support reproducing the emergence of opinion polarization concerning credit and reputation. By replacing the information content with other topics, the discussed emerge process can be generalized to other kinds of opinion polarization as well.

## 5 Discussion

The current research pursues a formal analysis of the evolution of information content when information diffuses in complex networks. Our key findings glance at the possible laws governing the dynamic evolution of information content: although information diffusion between individuals frequently involves random distortion, specific information invariants, whose quantity is bound by information selectivity characteristics in the network, are more likely to dominate

the diffused information content. Any information that is not invariant will be distorted gradually, whose speed is determined by the diversity of information selectivity in the network. A particular case of such distortion that frequently occurs is dissipation, corresponding to reducing information quantity. These global laws can be observed on a network scale or along the diffusion pathway, coexisting with the stochastic distortion between individuals. Their existences do not critically rely on noise, yet noise can intensify or disturb them.

The discovery of these potential laws begins with a formalization of the dynamics of information content utilizing the combination of network dynamics and information theory. The presented network dynamics offers a general description of the information-related interactions between individuals rather than constrained by specific information propagation models. It concentrates on the process during which each individual attempts to learn about the factual information based on the received information. Although individuals try to maintain the ground truth content while passing on the information, random distortion still originates from the confusion relations between contents [40]. Building on Shannon's theory [40], we have demonstrated that the distortion and dissipation processes will inevitably emerge if the information content consists of not only information invariants. The maximum information rates of these invariants are limited by the upper bound, which has been mathematically and computationally validated as optimal. Throughout the analysis, we have distinguished these properties from the effects of noise during information diffusion, proving that the existence of information distortion and dissipation is inherently determined by the information selectivity patterns in complex networks. The speeds of information distortion and dissipation are shaped by the diversity of information selectivity in networks and might be accelerated by noises. Taken together, the theoretical framework depicted here offers a natural interpretation for the characteristics of information evolution during diffusion.

To demonstrate the generalization capacity of our discovered laws and understand their connections with other scientific phenomena, we analyze information evolution in concrete biological and social systems. The principle that guides us through our computational experiments is to limit assumptions and explore whether complex biological or social phenomena can emerge spontaneously during information evolution. We begin by studying the origin of neural tuning properties in the V1 and MT cortices of the animal brain. Our experiment demonstrates that the neural selectivity variation process from V1 simple and complex neurons to MT neurons can be reproduced even when we only preset the tuning properties of simple neurons. For all types of neurons, their response attributes to stimuli have close relations to the upper bound of information invariants. The emergence of the neural selectivity of complex and MT neurons is a natural consequence of information distortion along the neural pathway because the response variances of these neurons are modified by the distortion situations in their cascade receptive fields. Then, we turn to explore the opinion polarization and the emergence of extreme views in social systems as another instance. We contextualize our analysis under the content of credit information. We suggest that information diffusion characteristics alone are sufficient to reproduce the opinion polarization process among agents. In our results, opinion polarization happens along with information dissipation. The dissipated information content enhances the monotonousness of opinions and widens the gap between different opinions. Extreme views gradually emerge in the social network as information dissipates, and one can see the increasing divergence among agents. In summary, these two computational experiments demonstrate the potential of our theory in practical applications and help us glance at the fundamental roles of information evolution in shaping biological and social systems on multiple scales.

Finally, a significant question for future exploration is how information distortion and dissipation are reduced when individuals in the complex network optimize the estimation of the factual information content. In realistic biological and social iterations, individuals have a strong tendency to enable themselves to learn about information as efficiently as possible. The optimization of the factual information estimation approach might further enable individuals to de-correlate between information content (control the confusion relations) and raise the upper bound of information invariants. Therefore, it would be meaningful to go further into the intricate effects of individuals' active behaviors on information evolution.

## Acknowledgements

This project is supported by the Artificial and General Intelligence Research Program of Guo Qiang Research Institute at Tsinghua University (2020GQG1017) as well as the Tsinghua University Initiative Scientific Research Program.

## References

- [1] Edward H Adelson and J Anthony Movshon. Phenomenal coherence of moving visual patterns. *Nature*, 300(5892):523–525, 1982.
- [2] Rudolf Ahlswede. A note on the existence of the weak capacity for channels with arbitrarily varying channel probability functions and its relation to shannon's zero error capacity. *The Annals of Mathematical Statistics*,

- 41(3):1027–1033, 1970.
- [3] Eralp Abdurrahim Akkoyunlu. The enumeration of maximal cliques of large graphs. *SIAM Journal on Computing*, 2(1):1–6, 1973.
- [4] Réka Albert and Albert-László Barabási. Statistical mechanics of complex networks. *Reviews of modern physics*, 74(1):47, 2002.
- [5] Lars Backstrom, Dan Huttenlocher, Jon Kleinberg, and Xiangyang Lan. Group formation in large social networks: membership, growth, and evolution. In *Proceedings of the 12th ACM SIGKDD international conference on Knowledge discovery and data mining*, pages 44–54, 2006.
- [6] Eytan Bakshy, Itamar Rosenn, Cameron Marlow, and Lada Adamic. The role of social networks in information diffusion. In *Proceedings of the 21st international conference on World Wide Web*, pages 519–528, 2012.
- [7] Rinni Bhansali and Laura P Schaposnik. A trust model for spreading gossip in social networks: a multi-type bootstrap percolation model. *Proceedings of the Royal Society A*, 476(2235):20190826, 2020.
- [8] Coen Bron and Joep Kerbosch. Algorithm 457: finding all cliques of an undirected graph. *Communications of the ACM*, 16(9):575–577, 1973.
- [9] Peter J Cameron. The random graph. *The Mathematics of Paul Erdős II*, pages 333–351, 1997.
- [10] Arthur Campbell. Word-of-mouth communication and percolation in social networks. *American Economic Review*, 103(6):2466–98, 2013.
- [11] Daryl J Daley and David G Kendall. Epidemics and rumours. *Nature*, 204(4963):1118–1118, 1964.
- [12] Pranav Dandekar, Ashish Goel, and David T Lee. Biased assimilation, homophily, and the dynamics of polarization. *Proceedings of the National Academy of Sciences*, 110(15):5791–5796, 2013.
- [13] Paul Erdős and Alfréd Rényi. On the evolution of random graphs. *Publ. Math. Inst. Hung. Acad. Sci*, 5(1):17–60, 1960.
- [14] Zachary Fulker, Patrick Forber, Rory Smead, and Christoph Riedl. Spite is contagious in dynamic networks. *Nature communications*, 12(1):1–9, 2021.
- [15] Andy Gardner and Stuart A West. Spite and the scale of competition. *Journal of evolutionary biology*, 17(6):1195–1203, 2004.
- [16] William Goffman and V Newill. Generalization of epidemic theory. *Nature*, 204(4955):225–228, 1964.
- [17] Jacob Goldenberg, Barak Libai, and Eitan Muller. Talk of the network: A complex systems look at the underlying process of word-of-mouth. *Marketing letters*, 12(3):211–223, 2001.
- [18] Jacob Goldenberg, Barak Libai, and Eitan Muller. Using complex systems analysis to advance marketing theory development: Modeling heterogeneity effects on new product growth through stochastic cellular automata. *Academy of Marketing Science Review*, 9(3):1–18, 2001.
- [19] Mark Granovetter. Threshold models of collective behavior. *American journal of sociology*, 83(6):1420–1443, 1978.
- [20] William D Hamilton. Selfish and spiteful behaviour in an evolutionary model. *Nature*, 228(5277):1218–1220, 1970.
- [21] Richard W Hamming. Error detecting and error correcting codes. *The Bell system technical journal*, 29(2):147–160, 1950.
- [22] Alumit Ishai, Leslie G Ungerleider, Alex Martin, Jennifer L Schouten, and James V Haxby. Distributed representation of objects in the human ventral visual pathway. *Proceedings of the National Academy of Sciences*, 96(16):9379–9384, 1999.
- [23] David Kempe, Jon Kleinberg, and Éva Tardos. Maximizing the spread of influence through a social network. In *Proceedings of the ninth ACM SIGKDD international conference on Knowledge discovery and data mining*, pages 137–146, 2003.
- [24] David M Kreps. *Game theory and economic modelling*. Oxford University Press, 1990.
- [25] Jure Leskovec, Lada A Adamic, and Bernardo A Huberman. The dynamics of viral marketing. *ACM Transactions on the Web (TWEB)*, 1(1):5–es, 2007.
- [26] Harry R Lewis. Computers and intractability. a guide to the theory of np-completeness, 1983.
- [27] Charles G Lord, Lee Ross, and Mark R Lepper. Biased assimilation and attitude polarization: The effects of prior theories on subsequently considered evidence. *Journal of personality and social psychology*, 37(11):2098, 1979.

- [28] László Lovász. On the shannon capacity of a graph. *IEEE Transactions on Information theory*, 25(1):1–7, 1979.
- [29] Akira Okubo and Smon A Levin. *Diffusion and ecological problems: modern perspectives*, volume 14. Springer Science & Business Media, 2013.
- [30] Romualdo Pastor-Satorras, Claudio Castellano, Piet Van Mieghem, and Alessandro Vespignani. Epidemic processes in complex networks. *Reviews of modern physics*, 87(3):925, 2015.
- [31] Romualdo Pastor-Satorras and Alessandro Vespignani. Epidemic spreading in scale-free networks. *Physical review letters*, 86(14):3200, 2001.
- [32] Matthew Richardson and Pedro Domingos. Mining knowledge-sharing sites for viral marketing. In *Proceedings of the eighth ACM SIGKDD international conference on Knowledge discovery and data mining*, pages 61–70, 2002.
- [33] Dario L Ringach, CE Bredfeldt, RM Shapley, and MJ Hawken. Suppression of neural responses to nonoptimal stimuli correlates with tuning selectivity in macaque v1. *Journal of Neurophysiology*, 87(2):1018–1027, 2002.
- [34] Dario L Ringach, Robert M Shapley, and Michael J Hawken. Orientation selectivity in macaque v1: diversity and laminar dependence. *Journal of Neuroscience*, 22(13):5639–5651, 2002.
- [35] Everett M Rogers. *Diffusion of innovations*. Simon and Schuster, 2010.
- [36] Nicole C Rust, Valerio Mante, Eero P Simoncelli, and J Anthony Movshon. How mt cells analyze the motion of visual patterns. *Nature neuroscience*, 9(11):1421–1431, 2006.
- [37] Kazumi Saito, Masahiro Kimura, Kouzou Ohara, and Hiroshi Motoda. Learning continuous-time information diffusion model for social behavioral data analysis. In *Asian Conference on Machine Learning*, pages 322–337. Springer, 2009.
- [38] Kazumi Saito, Ryohei Nakano, and Masahiro Kimura. Prediction of information diffusion probabilities for independent cascade model. In *International conference on knowledge-based and intelligent information and engineering systems*, pages 67–75. Springer, 2008.
- [39] Thomas C Schelling. Dynamic models of segregation. *Journal of mathematical sociology*, 1(2):143–186, 1971.
- [40] Claude Shannon. The zero error capacity of a noisy channel. *IRE Transactions on Information Theory*, 2(3):8–19, 1956.
- [41] Eero Simoncelli, WD Bair, JR Cavagnaugh, and J Anthony Movshon. Testing and refining a computational model of neural responses in area mt. *Investigative Ophthalmology and Visual Science*, 37(3), 1996.
- [42] Eero Simoncelli and David Heeger. A velocity representation model for mt cells. *Investigative Ophthalmology and Visual Science Supplement*, 35:1827, 1994.
- [43] Eero P Simoncelli and David J Heeger. A model of neuronal responses in visual area mt. *Vision research*, 38(5):743–761, 1998.
- [44] Robert J Snowden, Stefan Treue, Roger G Erickson, and Richard A Andersen. The response of area mt and v1 neurons to transparent motion. *Journal of Neuroscience*, 11(9):2768–2785, 1991.
- [45] Yang Tian and Pei Sun. Characteristics of the neural coding of causality. *Physical Review E*, 103(1):012406, 2021.
- [46] David C Van Essen and John HR Maunsell. Hierarchical organization and functional streams in the visual cortex. *Trends in neurosciences*, 6:370–375, 1983.
- [47] Duncan J Watts. A simple model of global cascades on random networks. *Proceedings of the National Academy of Sciences*, 99(9):5766–5771, 2002.
- [48] Keith Weigelt and Colin Camerer. Reputation and corporate strategy: A review of recent theory and applications. *Strategic management journal*, 9(5):443–454, 1988.
- [49] Zi-Ke Zhang, Chuang Liu, Xiu-Xiu Zhan, Xin Lu, Chu-Xu Zhang, and Yi-Cheng Zhang. Dynamics of information diffusion and its applications on complex networks. *Physics Reports*, 651:1–34, 2016.

## A Complex networks and individuals

All complex networks in our research are defined as connected random graphs utilizing the standard approach introduced by Erdős and Rényi [13, 9]. For convenience, the average degree of each random network is randomized as  $\langle \deg \rangle \in [5, 20]$ . In most cases, there is no restriction on the local topology characteristics of a random network during initialization (the only exception is the neural cluster used in our neuroscience experiment, where we design the network topology with realistic neural settings).

Information diffusion starts from a set of randomly selected individuals and gradually traverses all individuals in the network. For individual  $j$  who receives information indirectly, we quantify the time delay of information diffusion as  $\eta(j) = \langle \varphi[\mathcal{W}(i \rightarrow j)] \rangle_j$ , where  $\mathcal{W}(i \rightarrow j)$  is the shortest path from  $i$  to  $j$ , notion  $\langle \cdot \rangle_i$  measures the expectation value by traversing every individual  $i$  that receives factual information directly, and  $\varphi(\cdot)$  denotes the time delay weighting mapping. Our research uses a simplified definition  $\varphi[\mathcal{W}(i \rightarrow j)] = |\mathcal{W}(i \rightarrow j)|$ , meaning that the information diffusion between two neighbors costs a duration of 1 and the time cost on a path equals the path length.

Every individual in the complex network has its information selectivity, which can be principally described by  $\mathcal{P}(s_x | s_y)$ . Information selectivity is free to be applied in modeling preference, strategy, and other individualities. Except for the neuroscience experiment where we design the randomization of  $\mathcal{P}(s_x | s_y)$  with neural characteristics, the randomization in common cases is implemented without any restriction. The information selectivity properties of any two individuals in a complex network are not necessarily same. Therefore, the network can be either homogeneous or heterogeneous.

The process for an individual to estimate the factual information based on the received information is defined by a naive Bayesian inference, namely  $\mathcal{P}(s_y | s_x) \propto \mathcal{P}(s_x | s_y) \mathcal{P}(s_y) \mathcal{P}(s_x)^{-1}$ . The estimated factual information by individual  $j$  represents the beliefs of  $j$  on the ground truth information content.

In summary, information diffusion refers to a process where each individual receives information and passes on its response following information selectivity. Meanwhile, this individual attempts to learn about the factual information received by previous individuals. Please note that the passed-on response can be either same as (e.g., when this individual transmits what it knows) or different from (e.g., when this individual does not share its knowledge directly) the learned factual information. This property of practical significance can be implemented based on information selectivity. While analyzing information content variations during diffusion, what we measure is the dynamics of the learned factual information by individuals.

## B Probabilistic and graphical descriptions of information confusion

In the main text, we have sketched confusion relations from probabilistic and graphical perspectives. Here we elaborate the detailed definitions.

Let us consider a finite symbol set  $\mathcal{S}$ . We define that two symbols  $s_x, s_y \in \mathcal{S}$  are confused with each other if they may lead to the same response  $s_z \in \mathcal{S}$  of a certain individual  $i$ . From the probabilistic aspect, this condition requires  $\mathcal{P}_i(s_z | s_x) \in (0, 1]$  and  $\mathcal{P}_i(s_z | s_y) \in (0, 1]$ . After receiving response  $s_z$  from individual  $i$  (this means  $\mathcal{P}(s_z) = 1$ , implying  $\mathcal{P}_i(s_x | s_z) \in (0, 1)$  and  $\mathcal{P}_i(s_y | s_z) \in (0, 1)$ ), individual  $j$  can not confirm which symbol causes this response if there is no other information. Therefore, there is no confusion relation between symbols  $s_x$  and  $s_y$  when the response is  $s_z$  if

$$\{\mathcal{P}(s_x | s_z), \mathcal{P}(s_y | s_z)\} \cap \{0, 1\} \neq \emptyset. \quad (3)$$

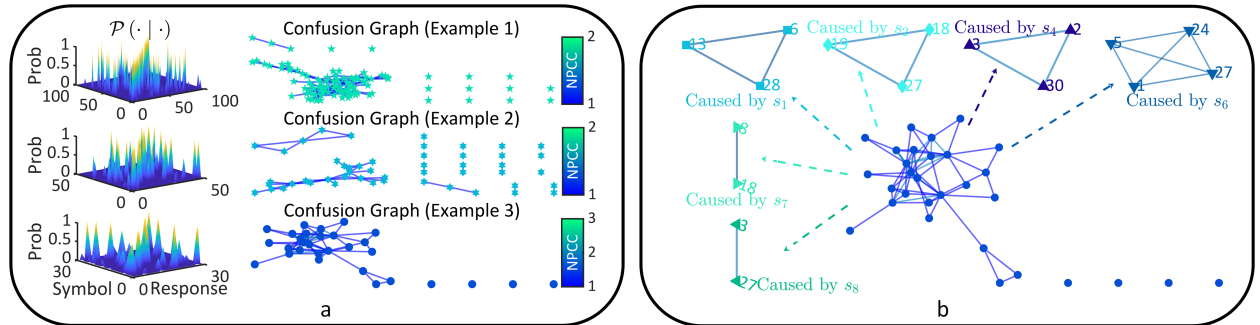
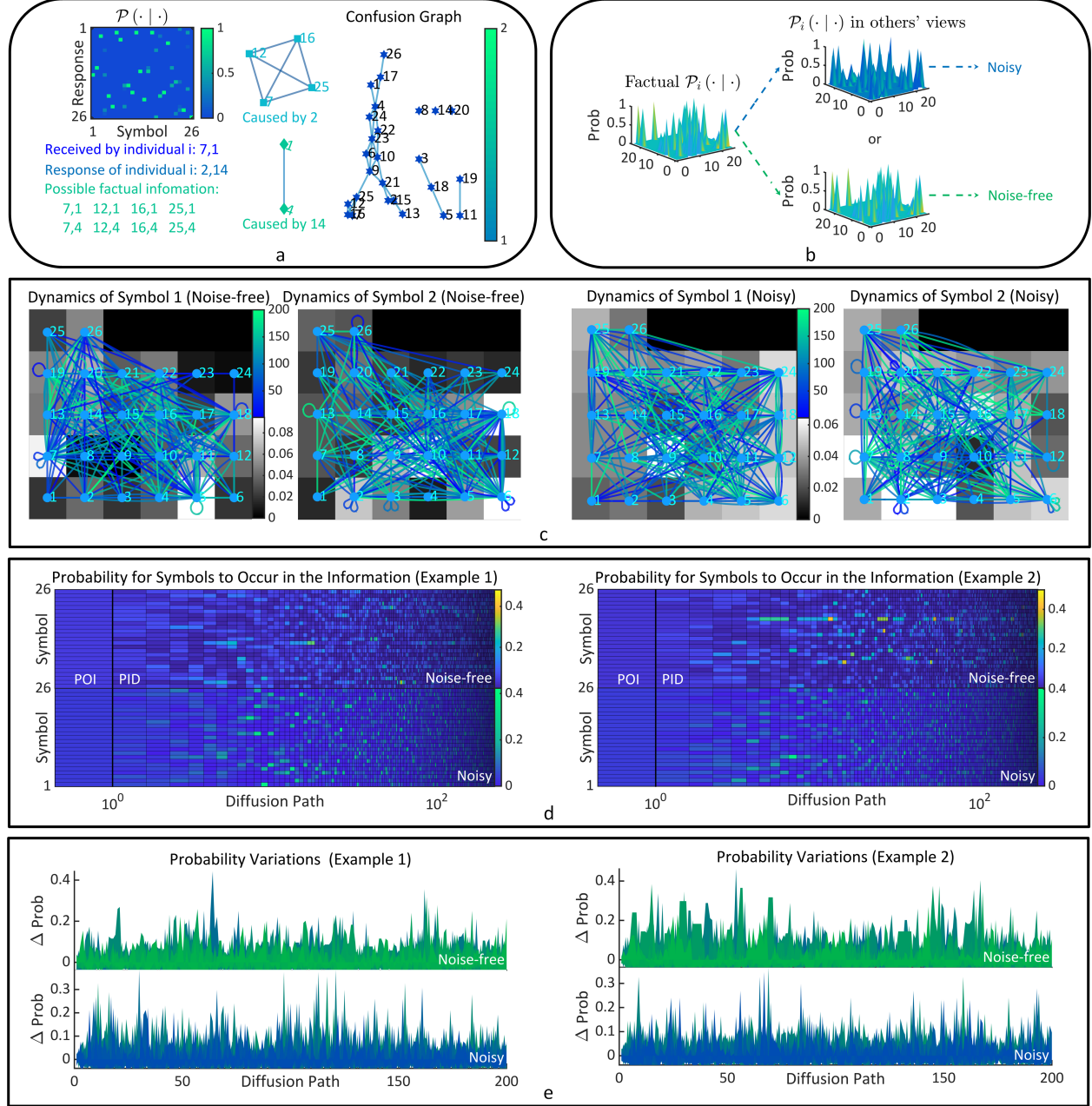


Figure 6: **Information confusion.** **a**, Here we illustrate 3 examples of probability distribution  $\mathcal{P}(\cdot | \cdot)$  on a symbol set  $\mathcal{S}$  of  $k$  symbols (here  $k \in \{100, 50, 30\}$ ). One can see the cases where  $\mathcal{P}(\cdot | \cdot) = 1$  or  $\mathcal{P}(\cdot | \cdot) = 0$  (non-confusion) and the cases where  $\mathcal{P}(\cdot | \cdot) \in (0, 1)$  (confusion). Correspondingly, we visualize the confusion graph, where each edge scales based on the number of possible confusion cases (NPCC). For instance, NPCC =  $n$  for edge  $(s_x, s_y)$  means that the confusion relation between symbols  $s_x$  and  $s_y$  might be caused by  $n$  kinds of responses. **b**, When the response has been specified, one can find all the confusion relations caused by this response.

Assuming that individual  $j$  attempts to estimate what individual  $i$  receives, then symbol  $s_x$  may be recognized as symbol  $s_y$ . This misrecognition between symbols, or referred to as information confusion, is studied by Shannon from the graphical perspective [40]. Specifically, Shannon represents symbols by the nodes in graph  $\mathcal{G}(\mathcal{S})$  and defines an



**Figure 7: Information distortion.** **a**, We illustrate an example where information confusion may lead to the distortion of information content. **b**, Two kinds of information diffusion are defined in our research. The first one requires the information selectivity of each individual to be completely known (noise-free diffusion) while the second kind does not (noisy diffusion). **c**, We randomize a piece of information consisting of uniformly distributed 26 symbols and let it diffuse in a chain of 200 individuals. Then, we visualize the dynamics of two symbols in the factual information content. These symbols change along the diffusion pathway (see the digraphs in color), transforming into other symbols with specific probability (see the background matrices in gray). **d**, The probability for each symbol to occur in the information content changes from its initial quantity (POI) to other quantities during diffusion (PID). **e**, Correspondingly, we calculate the difference between PID and POI.

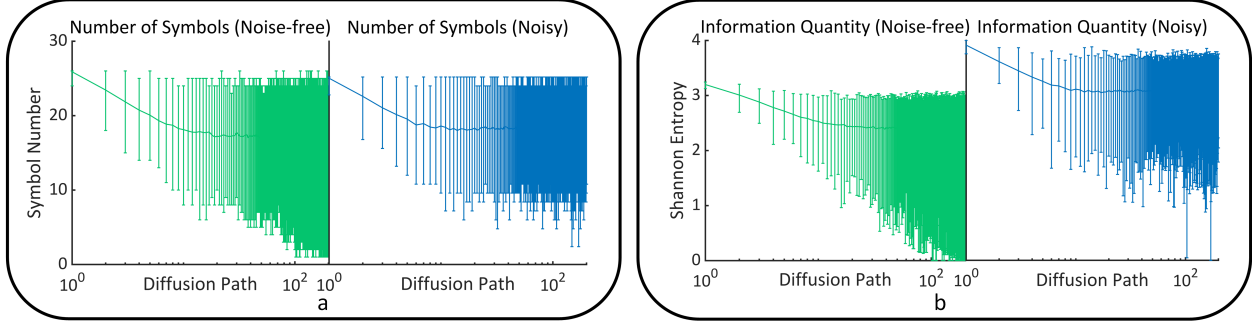


Figure 8: **Information dissipation.** **a**, The results of symbol counting indicate the decreasing process of the diversity of symbols in information content during diffusion. **b**, Correspondingly, one can see that the information quantity contained in information content decreases as well.

edge between two nodes if there is a confusion relation. Our research builds on Shannon's work and further distinguish between different types of confusion relations based on their corresponding causes (see Fig. 6).

### C Information distortion

Assume that there exist information confusion phenomena caused by the information selectivity of an individual. From other individuals' perspectives, information confusion creates multiple possibilities when they attempt to learn about the factual information received by the previous individual (see Fig. 7a). Without other auxiliary clues, these individuals might misestimate the factual information, leading to information content variation. This phenomenon is referred to as information distortion in our research. Please note that the noise during information transmission is excluded in the above analysis, implying that the existence of information distortion is independent of noise. Taking noise into consideration, we can further distinguish between noise-free and noisy information diffusion and compare information distortion during these two kinds of processes (see Fig. 7b).

Here we show several distortion processes of the symbols in information content, where one can see the transformation of the original symbols to other symbols due to misestimation (see Fig. 7c). Meanwhile, we also illustrate the dynamics of the probability for each symbol to occur in the information, indicating the effects of information distortion on information content during diffusion (see Fig. 7d-e).

### D Information dissipation

In our research, we define information dissipation as a kind of distortion process where the maximum number of symbols that possibly occur in the diffused information, or the maximum information quantities possibly contained in the diffused information, gradually decreases.

During information diffusion, the original probability distribution of symbols in the information content experiences complex changes (e.g., see Fig. 7d). This variation process usually behaves as decreasing. In SFig. 8, we implement symbol counting and information quantity measurement during the experiment in Fig. 7 to demonstrate the existence of information dissipation.

### E Confusion graph reconstruction during estimation

As described in our main text and Appendix A, the process for other individuals to learn (or estimate) the factual information received by individual  $i$  based on its response  $I_i = (s_1^i, \dots, s_l^i)$  virtually requires getting knowledge of the information selectivity of individual  $i$  (e.g.,  $\mathcal{P}_i(\cdot | \cdot)$  or  $\mathcal{G}_i(\mathcal{S})$ ). In a graphical perspective, this estimation is equivalent to a subdivided reconstruction of confusion graph  $\mathcal{G}_i(\mathcal{S})$ . For each symbol  $s_j^i$  in the response, the corresponding reconstructed graph  $\mathcal{G}_i(\mathcal{S} | s_j^i)$  only contains the confusion relations caused by this symbol (e.g., see Fig. 9a).

Considering the potential noise during diffusion, we can further define  $\mathcal{G}_i(\mathcal{S} | s_j^i) + \varepsilon$  to fit in with noisy information diffusion. Here  $\varepsilon$  measures the noise and vanishes in the noise-free case. Our research suggests that the confusion graph  $\mathcal{G}_i(\mathcal{S} | s_j^i)$  in other individuals' views may not be the same as the factual one due to noises (e.g., see Fig. 9b). The factual confusion graph governs the actual information diffusion process while the imaginary one affects other

individuals' behaviours. Therefore, the topology information of these two confusion graphs should be both taken into consideration. Specifically, we define

$$E[\mathcal{G}_i(\mathcal{S} | s_j^i) + \varepsilon] = \left\{ (s, s') \mid \mathcal{W}(s \rightarrow s') \in W[\mathcal{G}_i(\mathcal{S} | s_j^i)] \cup W[\widehat{\mathcal{G}}_i(\mathcal{S} | s_j^i)] \right\}, \quad (4)$$

where  $\widehat{\mathcal{G}}$  stands for the prediction of confusion graph  $\mathcal{G}$ , notion  $E(\cdot)$  denotes the edge set, and  $W(\cdot)$  denotes the path set (see **Fig. 9b**).

We further generalize the confusion graphs of symbols to the confusion graphs of strings following Shannon's idea [40]. Our generalization is implemented based on the graph product  $\boxtimes$  (e.g., see **Fig. 9c**). The precondition for any two tuples  $(s_p, s_q), (s_b, s_d) \in \mathcal{S} \times \mathcal{S}$  to be connected in the graph product  $\mathcal{G}_i(\mathcal{S} | s_j^i) \boxtimes \mathcal{G}_i(\mathcal{S} | s_j^i)$  is one of the following cases:

- $s_p = s_b$  and  $s_q$  is connected with  $s_d$  in graph  $\mathcal{G}_i(\mathcal{S} | s_j^i)$ ;
- $s_q = s_d$  and  $s_p$  is connected with  $s_b$  in graph  $\mathcal{G}_i(\mathcal{S} | s_j^i)$ ;
- $s_p$  and  $s_q$  are respectively connected with  $s_b$  and  $s_d$  in graph  $\mathcal{G}_i(\mathcal{S} | s_j^i)$ .

This generalization allows to define

$$\mathcal{G}_i(\mathcal{S} | s_j^i)^n = \mathcal{G}_i(\mathcal{S} | s_j^i) \boxtimes \dots \boxtimes \mathcal{G}_i(\mathcal{S} | s_j^i), \quad (5)$$

representing the confusion relations between strings of length  $n$  (e.g., see **Fig. 9c**).

## F Upper bound of information invariants

In our main text, we have formalized the maximum amount of information (no matter if it is a symbol or string) that can diffuse from individual  $i$  to other individuals without confusion given a response  $s_j^i$

$$\Theta(i \rightarrow i+1 | s_j^i) = \sup_{n \in \mathbb{N}} \log \sqrt[n]{\alpha[(\mathcal{G}_i(\mathcal{S} | s_j^i) + \varepsilon)^n]}, \quad (6)$$

where  $\alpha(\cdot)$  denotes the independence number of confusion graph (cardinality of the largest independent set), measuring the maximum amount of the symbols that will not be confused given a response  $s_j^i$ . Equation (6) is firstly introduced in Shannon's work [40]. This definition helps explore what will be invariant during information diffusion.

A daunting challenge lies in that the analytic calculation of  $\Theta$  is principally difficult (e.g., Shannon failed to measure  $\Theta$  on 5-cycle [40]. This problem has remained unsolved until Lovász's work [28]). On the other hand, any computational attempt will inevitably meet obstacles because  $\alpha$  is  $NP$ -hard to compute [26]. We have built on Shannon's work [40] to estimate the upper bound of  $\Theta$

$$\Theta(i \rightarrow i+1 | s_j^i) \leq \log \left[ \frac{\theta + \theta \sum_s (1 - \tau_s)}{\mu} \right]^\omega |\mathcal{S}|^{(1-\omega)}, \quad (7)$$

where notion  $\tau_s = \mathcal{U}[\deg(s)]$  traverses all nodes in graph  $\mathcal{G}_i(\mathcal{S} | s_j^i) + \varepsilon$  (here  $\mathcal{U}(\cdot)$  is the unit step function). And we mark that  $\omega = \mathcal{U}(\sum_s \tau_s)$ . Moreover, we pick one node that has minimum degree in the graph. Then  $\mu$  measures the number of the cliques that contain this node and  $\theta$  counts the cliques in the same connected component with this node.

Here we elaborate all the detailed derivations of the upper bound (7).

### F.1 Derivations of the upper bound

Our derivations begin with an important property discovered by Shannon and subsequent researchers [40, 28]

$$\log \alpha[\mathcal{G}_i(\mathcal{S} | s_j^i) + \varepsilon] \leq \Theta \leq \log \lambda[\mathcal{G}_i(\mathcal{S} | s_j^i) + \varepsilon]^{-1}. \quad (8)$$

Here  $\lambda(\cdot)$  denotes the maximum clique value

$$\lambda[\mathcal{G}_i(\mathcal{S} | s_j^i) + \varepsilon] = \min_{\mathcal{X}} \max_{\mathcal{K} \in K} \sum_{s \in \mathcal{K}} X_s, \quad (9)$$

where  $\mathcal{X}$  is an arbitrary random distribution  $\mathcal{X} = \{X_s \mid s \in \mathcal{S}\}$ , and  $K$  denotes the clique set of confusion graph  $\mathcal{G}_i(\mathcal{S} | s_j^i) + \varepsilon$  (a clique  $\mathcal{K}$  is a complete sub-graph).

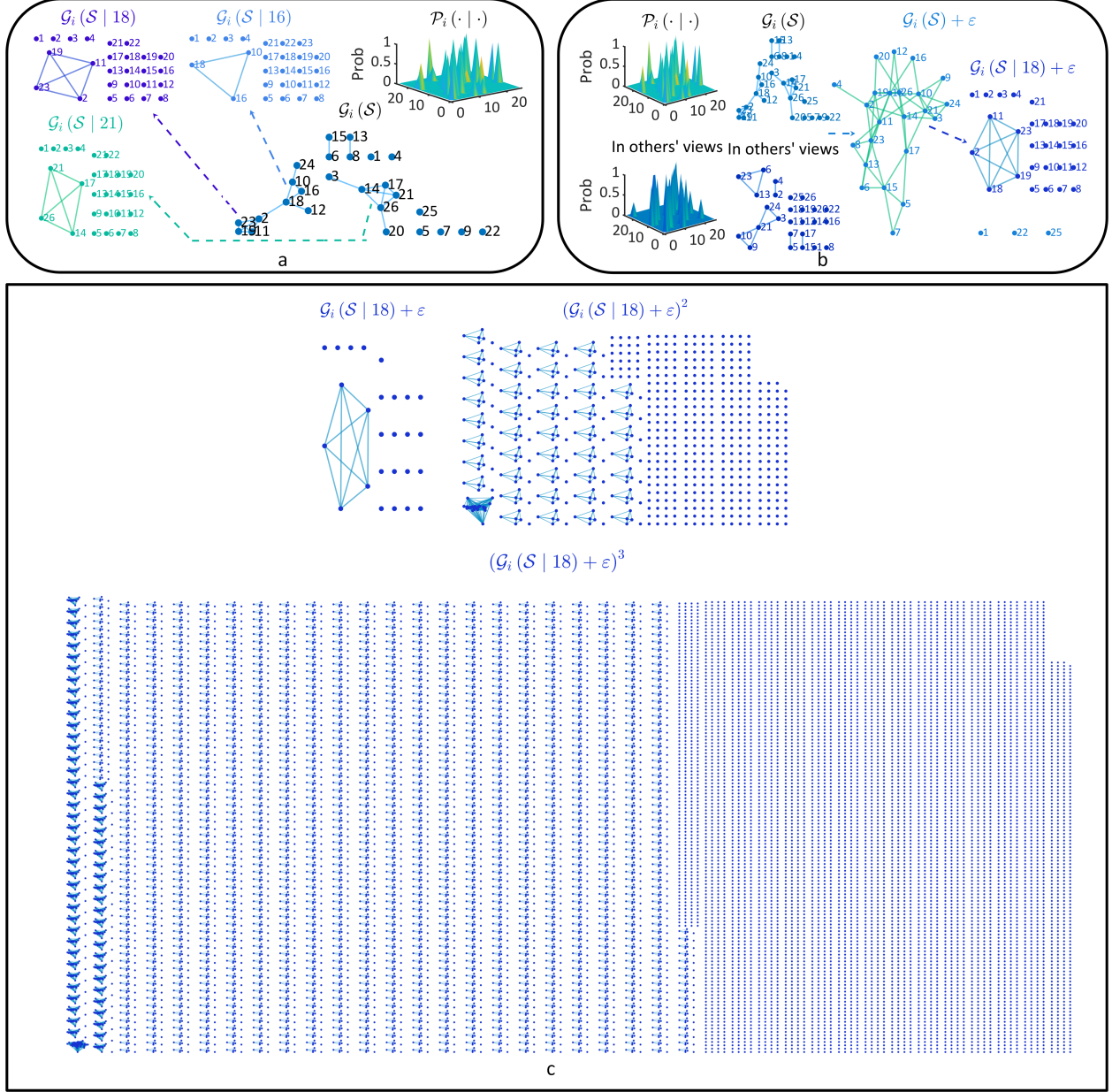


**Figure 9: Confusion graph reconstruction.** **a**, We illustrate several reconstructed confusion graphs  $\mathcal{G}_i(\mathcal{S} | \cdot)$  caused by specific responses of individual  $i$ . **b**, We show how  $\mathcal{G}_i(\mathcal{S}) + \varepsilon$  and  $\mathcal{G}_i(\mathcal{S} | \cdot) + \varepsilon$  inherit topology information from the ground truth confusion graph  $\mathcal{G}_i(\mathcal{S})$  and the confusion graph in other individuals' views. **c**, We illustrate the graph products of a reconstructed confusion graph up to 3-order.

Although it is non-trivial to calculate  $\Theta$  directly, we can still obtain a bound of  $\Theta$  based on inequality (8). We suggest that the maximum clique value  $\lambda$  satisfies

$$\lambda \geq \left[ \frac{\mu}{\theta + \theta \sum_s (1 - \tau_s)} \right]^\omega |\mathcal{S}|^{-(1-\omega)}. \quad (10)$$

One can immediately realize that the upper bound of  $\Theta$  in (7) is derived from the combination of (8) and (10). Therefore, the validity of (7) can be ensured by proving (10).

Considering the value of  $\omega$ , we can subdivide (10) into two cases:

- The first case corresponds to  $\omega = 1$ , or equivalently, meaning that  $E [\mathcal{G}_i (\mathcal{S} | s_j^i) + \varepsilon] \neq \emptyset$ . One can see that (10) can be reformulated as

$$\lambda \geq \frac{\mu}{\theta + \theta \sum_s (1 - \tau_s)}. \quad (11)$$

- The second case corresponds to  $\omega = 0$ , or equivalently, implying that  $E [\mathcal{G}_i (\mathcal{S} | s_j^i) + \varepsilon] = \emptyset$ . Under this condition, (10) is equivalent to

$$\lambda \geq \mathcal{S}^{-1}. \quad (12)$$

Given the above analysis, let us prove (11) and (12) respectively.

**In the first case**, we consider the dual problem of the definition of  $\lambda$

$$\lambda = \min_{\mathcal{X}} \max_{\mathcal{K} \in K} \sum_{s \in \mathcal{K}} X_s = \max_{\mathcal{Y}} \min_{s \in \mathcal{S}} \sum_{\mathcal{K} \ni s} Y_{\mathcal{K}}, \quad (13)$$

where  $\mathcal{Y}$  is an arbitrary random distribution  $\mathcal{Y} = \{Y_{\mathcal{K}} \mid \mathcal{K} \in K\}$ . Here the value assignment of  $\mathcal{Y}$  is implemented as following

- Assuming that  $\mathcal{G}_i (\mathcal{S} | s_j^i) + \varepsilon$  has  $m$  connected components in total, we assign  $m^{-1}$  to each connected component in  $\mathcal{G}_i (\mathcal{S} | s_j^i)$ . The number of connected components can be worked out by  $m = 1 + \sum_s (1 - \tau_s)$ ;
- In a connected component containing  $k$  cliques, we assign each clique as  $(km)^{-1}$ .

Based on the value assignment described above, it is easy to know

$$\lambda \geq \min_{s \in \mathcal{S}} \sum_{\mathcal{K} \ni s} Y_{\mathcal{K}} = \theta^{-1} \mu m^{-1}, \quad (14)$$

which can be reorganized as

$$\lambda \geq \mu \left[ \theta + \theta \sum_s (1 - \tau_s) \right]^{-1}. \quad (15)$$

Thus the validity of (10) under this condition is demonstrated.

**In the second case**, there exists no edge in  $\mathcal{G}_i (\mathcal{S} | s_j^i) + \varepsilon$ . Therefore, the maximum clique in this graph is each individual node itself. Following the value assignment method we use above, one can see

$$\lambda \leq \max_{\mathcal{K} \in K} \sum_{s \in \mathcal{K}} X_s = \theta^{-1} \mu m^{-1}, \quad (16)$$

$$\lambda \geq \min_{s \in \mathcal{S}} \sum_{\mathcal{K} \ni s} Y_{\mathcal{K}} = \theta^{-1} \mu m^{-1}, \quad (17)$$

where  $\mu = 1$ ,  $\theta = 1$  and  $m^{-1} = |\mathcal{S}|^{-1}$ . Thus, (10) is correct in this case.

In summary, we can safely derive the upper bound of  $\Theta$  in (7) based on (8) and (10).

## F.2 Optimality of the upper bound

Here we further prove that (7) is the supremum of  $\Theta$  during information diffusion if  $\mathcal{G}_i (\mathcal{S} | s_j^i) + \varepsilon$  is not a complete graph. In the opposite case,  $\Theta = 0$  can be directly obtained, making the upper bound estimation unnecessary.

If  $\mathcal{G}_i (\mathcal{S} | s_j^i) + \varepsilon$  is not a complete graph, then we know  $\sum_s \tau_s < |\mathcal{S}|$ , which can be subdivided into two cases

- $\sum_s \tau_s = 0$ , meaning that there is no edge in the graph. Under this condition, the biggest independent set in  $\mathcal{G}_i (\mathcal{S} | s_j^i) + \varepsilon$  is itself, implying that  $\alpha = |\mathcal{S}|$ . Based on (7), we know

$$\alpha = \lambda^{-1}. \quad (18)$$

Combined with (8), (18) implies

$$\nexists \delta > 0, \Theta + \delta \leq \log \lambda^{-1}. \quad (19)$$

Thus the upper bound in (7) is a supremum in this case.

- $0 < \sum_s \tau_s < |\mathcal{S}|$ , meaning that there is at least one isolated node in the graph. Being isolated, the node has the smallest degree 0. We know  $\mu = 1$  and  $\theta = 1$  under this condition. Then, (7) can be written as

$$\lambda^{-1} \leq 1 + \sum_s (1 - \tau_s), \quad (20)$$

where  $\sum_s (1 - \tau_s)$  measures the number of isolated nodes, and  $1 + \sum_s (1 - \tau_s)$  counts the number of connected components.

Because the maximum independent set contains only one node from each connected component, we can know  $\alpha = \lambda^{-1}$ . Following (19), we can prove that the upper bound is actually a supremum in this case.

To conclude, we know that when  $\mathcal{G}_i (\mathcal{S} | s_j^i) + \varepsilon$  is not a complete graph, the upper bound is a supremum.

## G Biological system experiment

As described in the main text, we attempt to explore the neural pathway from the primary visual cortex (V1) to the middle temporal visual cortex (MT) in the brain. The phenomenon of interest during information diffusion is that the neural selectivity (a kind of information selectivity that governs neural activity profile) changes from the selectivity of the velocity component orthogonal to the preferred spatial orientation (simple and complex neurons in V1 [1]) to the selectivity of velocity entirely (MT neurons [36]). Previous studies have demonstrated that this variation accounts for the subdivided and staged neural representation of motion information [36].

Computationally, Simoncelli and Heeger simulate the above process in a layered neural cluster model [43, 41, 42]. The cluster begins with a layer to compute the weighted sum of inputs in the linear receptive field of every simple neuron. Then, each complex neuron in the second layer responds to the weighted sum of the simple neuron afferents that are distributed within a specific spatial area and have the same orientation and phase. In the third layer, every MT neuron is driven by multiple complex neurons whose preferred orientations are consistent with the desired velocity. This model is generalized and experimentally-validated in a follow-up study [36].

To explore how the modeled phenomenon naturally emerges from neural collective dynamics during information diffusion, we randomize a tripartite neural cluster that is not strictly layered:

- The network topology of neural cluster is generated as following
  - We randomize three complex networks, corresponding to simple, complex, and MT neuron sub-clusters. Each network is a connected graph. The number of neurons is set as 10000, and the ratio between these three types of neurons approximates 6 : 3 : 1.
  - We randomly generate edges (synaptic connections) between the simple neuron sub-cluster and the complex neuron sub-cluster. About  $x\%$  of complex neurons feature such connections, and each of them connects with  $y$  simple neurons (here  $x \approx 80$  and  $y \in [15, 50]$ ). Similar settings are applied to generate edges between the complex neuron sub-cluster and the MT neuron sub-cluster as well. The probability for a MT neuron to connect with a simple neuron directly is set as  $\mathcal{P} \leq 10^{-3}$ .
- The neural activity profiles of three types of neurons are set as
  - The information selectivity of each simple neuron is randomized following neural realistic settings (e.g., receptive field and tuning curve [34, 33]). Specifically, the selectivity of each simple neuron is described by triangular orientation tuning curve

$$R(s) = \mathcal{U}(B - |s - \hat{s}|) r_{max} \left(1 - \frac{|s - \hat{s}|}{B}\right) + r_{min}, \quad (21)$$

where  $s \in [-90, 90]$  denotes the stimulus orientation, notion  $\hat{s}$  is the preferred orientation, parameter  $B \in (0, 180)$  measures the band width, and  $r_{max}, r_{min} \in [0, 1]$  respectively stand for the maximum and minimum response rates. As for complex and MT neurons, there is no preset limitation for their activity profiles.

- We characterize stimulus-triggered neural activities utilizing a non-homogeneous stochastic neural network [45], where we treat simple neurons as input neurons in the network to drive the whole neural cluster. This framework can generate variable neural activities governed by both neural selectivity and network dynamics (see **Fig. 10a** and **Fig. 10b**). One can find a systematic definition of it in [45].

Given the stimulus-triggered neural activities of our neural cluster, there are several parameters to calculate:

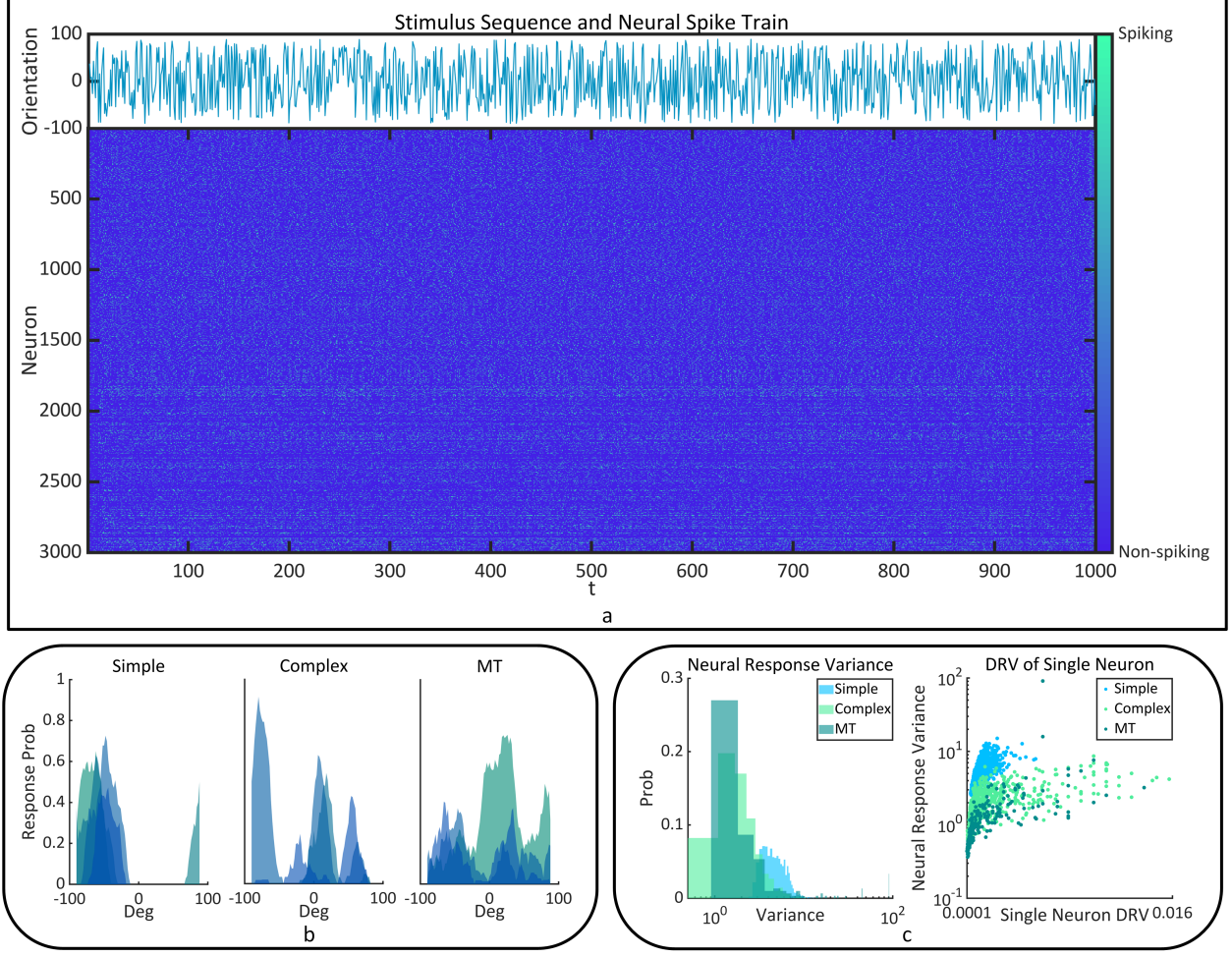


**Figure 10: Characteristics of neural activities.** **a**, The randomized stimulus sequence and the corresponding stimulus-triggered neural activities are shown. **b**, We illustrate 5 examples of  $\mathcal{P}$  (Response | Stimulus) for each kind of neurons, where one can qualitatively see the broadening process of neural selectivity from simple to MT neurons. **c**, We visualize the probability distributions of the variance of normalized neural response rates (left). One can find a positive correlation between this variance and the single neuron DRV. Similar phenomenon has been seen between the variance and the DRV in our main text.

- We count the response rate  $r_i(s)$  of each neuron  $N_i$  to every stimulus  $s$ . Then we define the normalized neural response rate as

$$\hat{r}_i(s) = r_i(s) \mathbb{E}_s(r_i(s))^{-1} \quad (22)$$

(here the expectation value acts as the normalization reference) and calculate its variance  $\text{Var}_s[\hat{r}_i(s)]$ . This variance principally measures the variability of neural responses to different stimuli. A larger response variability implies a narrower neural selectivity (see Fig. 9c);

- We estimate the neural response conditional probability as  $\mathcal{P}_i(\text{Spike} | s) \approx r_i(s) f^{-1}(s)$  (here  $f(\cdot)$  denotes frequency), based on which we measure  $\mathcal{P}_i(\text{Spike}, s) = \mathcal{P}_i(\text{Spike} | s) \mathcal{P}(s)$  and further define the determinability rate of neuron  $N_i$  to stimulus  $s$  as

$$\eta_i(s) = 1 - \mathcal{P}_i(\text{Spike}, s) \mathbb{E}_s[\mathcal{P}_i(\text{Spike}, s)]^{-1}. \quad (23)$$

By calculating the variance  $\text{Var}_s[\eta_i(s)]$ , we can quantify the capacity of neuron  $N_i$  to resist information distortion (referred to as single neuron DRV, see Fig. 10c). Here we do not concentrate on  $\text{Var}_s[\eta_i(s)]$  since its connection to the neural response variability  $\text{Var}_s[\hat{r}_i(s)]$  is trivial (one can immediately find the positive correlation between them). To implement non-trivial analyses, we define the determinability rate variance of neuron  $N_i$  as  $\mathbb{E}_{N_j}\{\text{Var}_s[\eta_i(s)]\}$ , where each  $N_j$  is a neuron located at specific diffusion paths from simple

neurons to neuron  $N_i$  (referred to as DRV). The non-triviality of this parameter lies in that it quantifies the capacity of the diffused information to resist distortion before neuron  $N_i$  receives the information. Therefore, there can be potential causal connections between the determinability rate variance and the neural selectivity of neuron  $N_i$  (see **Fig. 5b** in our main text).

## H Social system experiment

As described in the main text, we attempt to explore whether information diffusion characteristics alone are sufficient to polarize opinions in multi-agent interactions.

Without loss of generality, we implement the analysis based on the opinion concerning credit. In real financial, marketing, and other social activities, agents may do selfish (e.g., lie or cheat) or even spiteful (e.g., break rules for non-interest reasons) behaviors to make profits or harm others [20, 15]. These costly behaviors eventually lead to the damage on credit [14, 48, 24]. A widespread phenomenon concerning credit damage is the emergence of extreme views towards the credit of an agent. The opinions on credit tend to be polarized when credit information diffuses [12]. Although the agent occasionally does selfish or spiteful behaviors, its credit in others' view may still approach extraordinarily high or extremely low. This phenomenon may be caused by both psychological and physical factors [12, 27].

In our computational experiment, agent  $i$  does selfish or spiteful behaviors with probability of  $p'$  or  $p''$  in a  $l$ -run game, respectively. We implement the experiment in a complex network of 2000 agents 10 times. Each time we randomize the credit information as a string of length  $l = 300$ , consisting of indexes 1 (selfish), 2 (spiteful), and 3 (amicable). The proportion of each index in the information content represents the probability of corresponding behaviors, determining

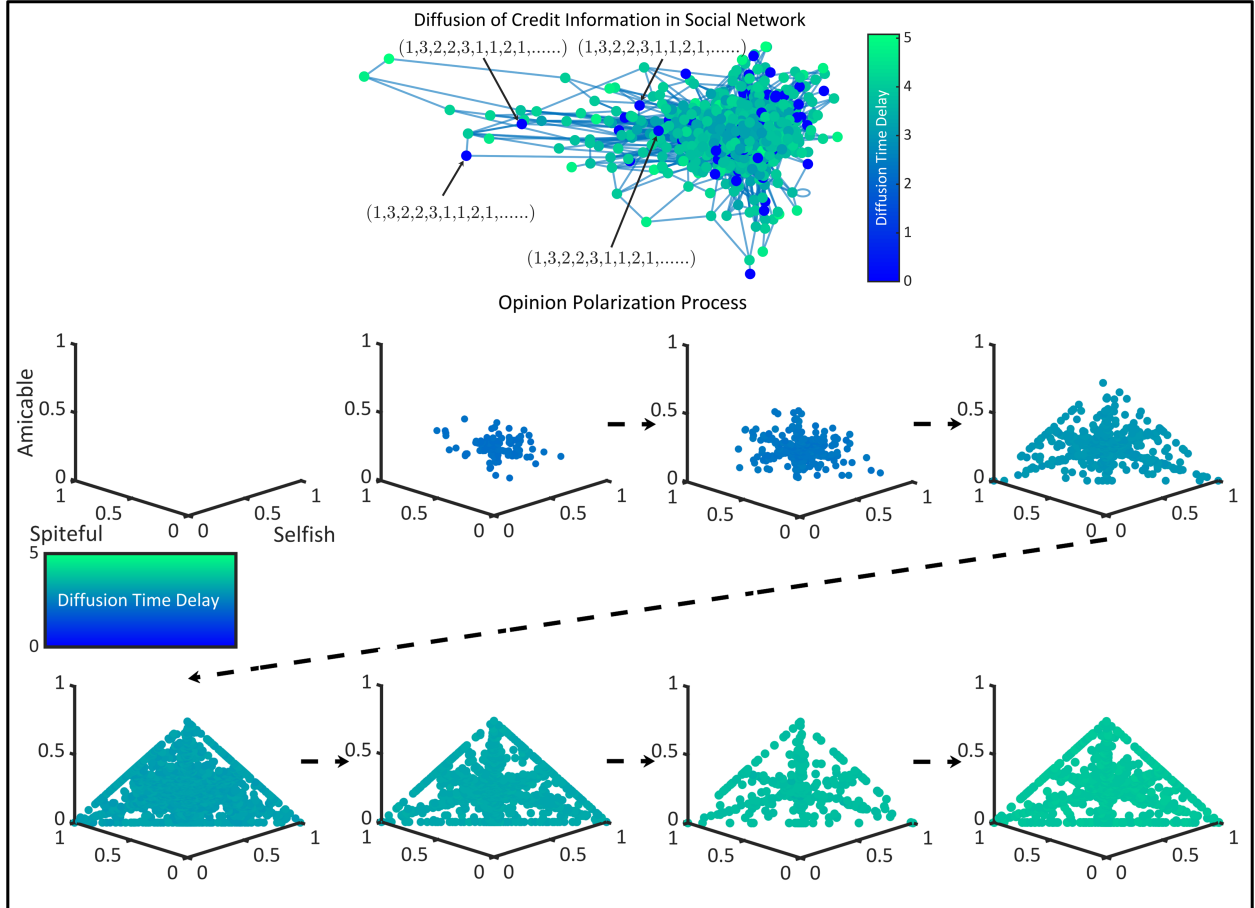


Figure 11: **Opinion polarization.** The opinion polarization process during the credit information diffusion in a social network. Here all data sets obtained in 10 times of experiments are included.

whether agent  $i$  will be treated as selfish, spiteful, or amicable. The credit information first arrives at  $m$  randomly selected agents ( $m \approx 200$ ) and then diffuses to other agents (see **Fig. 11**).

In our main text, the probability for agent  $i$  to do selfish or spiteful behaviors in the game is driven farther from  $p'$  or  $p''$  during information diffusion. It gradually approaches 0 or 1, suggesting that the opinion on the credit of agent  $i$  is polarized (see **Fig. 11**). To quantify the polarization degree of opinions, we define the opinion monotonousness as

$$\chi = \max_i \mathcal{P}_i - \text{secmax}_i \mathcal{P}_i, \quad (24)$$

where  $\mathcal{P}_i$  denotes the proportion of each index  $i$  in information content (here  $i \in \{1, 2, 3\}$ ), and operator  $\text{secmax}$  measures the second largest value. One can see that (24) quantifies the degree for a certain index  $i$  to surpass the other two indexes in proportion.

Moreover, we measure the proportion of extreme opinions among all opinions. Specifically, we treat an opinion as extreme if it characterizes the agent as a selfish, spiteful, or amicable person with a probability greater than 0.8 (in other words,  $\mathcal{P}_i > 0.8$ ).